

# INFRARED COLOURS OF STAR-FORMING GALAXIES AND A FLUX CALIBRATION OF ISOCAM ELAIS CATALOGUES

Petri Väisänen<sup>1</sup> and Thierry Morel<sup>2</sup>

<sup>1</sup>European Southern Observatory, Alonso de Cordova 3107, Vitacura, Casilla 19001, Santiago 19, Chile

<sup>2</sup>Osservatorio Astronomico di Palermo, Piazza del Parlamento 1, 90134 Palermo, Italy

## ABSTRACT

We present  $J$  and  $K$ -band near-infrared photometry of a sample of ISOCAM sources detected by the European Large Area  $ISO$ -Survey (ELAIS). All of the high-reliability LW2 ( $6.7\mu\text{m}$ ) sources and 80 per cent of the LW3 ( $15\mu\text{m}$ ) sources are identified in the near-IR survey reaching  $K \approx 17.5$  mag.

The near- to mid-IR flux ratios can effectively be used to separate stars from galaxies in mid-IR surveys: at  $6.7\mu\text{m}$ , 80 per cent of the identified ELAIS objects are stars while at  $15\mu\text{m}$  80 per cent are galaxies. The stars are then used to perform an accurate new calibration of the ELAIS ISOCAM data at both  $6.7$  and  $15\mu\text{m}$ : we adopt values of 1.23 and 1.05 ADU/gain/s/mJy for the LW2 and LW3 filters, respectively.

The ISOCAM ELAIS survey is found to mostly detect strongly star-forming late-type galaxies. We show that near to mid-IR colour-colour diagrams can be used to further classify galaxies, as well as study star-formation. In a  $[15/2.2]$  vs.  $[6.7/2.2]$  plot the Hubble type of a galaxy can be roughly estimated from its position along the diagonal ( $[6.7/15] = 1$ ) and the star-forming efficiency from a galaxy's departure from the diagonal (eg.  $[6.7/15] < 1$ ).

The ELAIS galaxies yield an average mid-IR flux ratio  $LW2/LW3 = 0.67 \pm 0.27$ . We discuss this  $[6.7/15]$  ratio as a star formation tracer using  $ISO$  and  $IRAS$  data of a local comparison sample. The  $[2.2/15]$  ratio is also found to be a good indicator of activity level in galaxies and conclude that the drop in the  $[6.7/15]$  ratio seen in strongly star-forming galaxies is a result of both an increase of  $15\mu\text{m}$  emission and an apparent depletion of  $6.7\mu\text{m}$  emission.

Key words: ISO – infrared: galaxies – surveys – infrared: stars

## 1. INTRODUCTION

To understand the history of luminous matter in the Universe it is necessary to study the infrared properties of galaxies. It is also important to tie together the physical processes seen at work in the ISM and stars of the nearby galaxies with the integrated properties of high-redshift galaxies. The European Large Area  $ISO$  Survey (ELAIS) stands as an important bridge between local and deep  $ISO$ -surveys.

The mid-infrared truly opened up for study only with the  $ISO$ -mission (see reviews by Genzel & Cesarsky 2000, Helou 1999). Many studies (eg. Mattila et al. 1999, Helou et al. 2000)

have confirmed the complex nature of spectral energy distributions of disk galaxies in the  $3 - 20\mu\text{m}$  range. In addition to a continuum due to hot or warm dust there are bright IR-bands in the MIR, often called the Unidentified Infrared Bands (UIBs) and proposed to be the signature of Polycyclic Aromatic Hydrocarbons (PAHs).

The PAHs are an essential component in forming the mid-infrared  $[6.7/15]$  colour ratio which is emerging as a tracer of star forming activity in galaxies (Vigroux et al. 1996, 1999, Sauvage et al. 1996, Dale et al. 2000, Roussel et al. 2001a). The value  $[6.7/15] \approx 1$  is expected in quiescent medium and PDRs, while HII regions have  $[6.7/15] < 0.5$  (eg. Cesarsky et al. 1996). The  $[6.7/15]$  ratio thus remains close to unity for quiescent and mildly star forming galaxies, while it starts to drop for those with more vigorous star formation activity.

A subset of the ISOCAM ELAIS survey with near-IR follow-up observations is presented here (see also Väisänen et al. 2002).

## 2. OBSERVATIONS AND DATA

The mid-IR ELAIS  $ISO$ -observations were made with the ISOCAM LW2 and LW3 filters; For a description of the observations, data reduction, and source extraction see Oliver et al. (2000) and Serjeant et al. (2000). The latest version of the source catalogue, the v.1.3 preliminary analysis was used – however, we considered only those detections with near-IR matches.

The  $J$  and  $K$ -band observations were carried out using the STELIRCam instrument at the 1.2-m telescope of the F. L. Whipple Observatory on Mount Hopkins (see Väisänen et al. (2000). The survey area is approximately 1 square degree, in two separate regions centered at

RA=16h 09m 00s, DEC=54°40'00" (N1) and

RA=16h 36m 00s, DEC=41°06'00" (N2).

## 3. ELAIS FLUX CALIBRATION

Most stars could be easily separated by their morphology. However, also the near to mid-IR colour can be used very effectively. Flux ratios of  $[2.2/15] > 10$  and  $[2.2/6.7] > 2$  were found to define stars (though if using only the latter limit some elliptical galaxies overlap with the stars).

The stars were used for a new and accurate flux calibration of the ELAIS  $ISO$ -data. The ELAIS catalogue v.1.3 merely uses a one-to-one conversion of ADUs/gain/s to mJy fluxes. B

and V-band bolometric magnitudes (Hipparcos, SIMBAD) of stars seen in the ELAIS fields had been used in previous attempts to calibrate the ELAIS fluxes. With good quality near-IR data we potentially have a better chance of deriving the calibration factor because the uncertainty of extrapolating optical magnitudes into mid-IR is greatly reduced.

From our own sample of stars we used only those with the highest mid-IR reliability flag, and in addition we excluded stars with  $K < 8$  mag because of saturation in the NIR images. The stars were compared to observationally based stellar spectra used for the extensive ISOCAM and ISOPHOT calibration programs<sup>1</sup>. We calculated near- and mid-IR colours of stars with a range of spectral types from these spectra, which are estimated to be accurate within 5 per cent. The mid-IR fluxes were colour-corrected according to *ISO*-convention.

Fig. 1a shows the stars detected at  $6.7\mu\text{m}$  plotted as  $[2.2/6.7]$  vs.  $J - K$ , with the model stars overplotted as solid symbols. Ignoring the negligible colour-term, from the average difference of  $[2.2/6.7]$  ratios of observations and models, we derive a correction factor of 1.22 to the  $6.7\mu\text{m}$  fluxes of the v.1.3 ELAIS catalogue.

Fig. 1b shows the equivalent plot for the  $15\mu\text{m}$  stars – there are much less stars here, but the overall calibration of the v.1.3 ELAIS catalogue appears quite accurate. We derive a 1.05 ADU/gain/s/mJy calibration for the LW3 data. The  $J$ -band data can be used as well: panels *c* and *d* show the equivalent colour-colour plots with  $J$ -band flux. The calibration factors are confirmed, as we find 1.24 and 1.06 ADU/gain/s/mJy for the LW2 and LW3 filters, respectively. We thus adopt values of 1.23 and 1.05 ADU/gain/s/mJy for the LW2 and LW3 filters.

Fig. 2 shows the *predicted*  $6.7$  and  $15\mu\text{m}$  stellar fluxes (derived from the observed  $K$ -magnitude and model colours) against the observed and re-calibrated ELAIS  $6.7$  and  $15\mu\text{m}$  fluxes. The scatter is seen to be very small, and the relation highly linear over two orders of magnitude. The conversion factors are in good agreement also with the ISOCAM handbook values of 2.32 and 1.96 ADU/gain/s/mJy (Blommaert 1998), where an additional factor of 2 correction for signal stabilization has been included. This lends strong support for the accuracy of the reduction and photometric techniques used in the creation of the ELAIS Preliminary catalogue.

## 4. RESULTS

### 4.1. IDENTIFICATIONS

Table 1 presents the summary of detected and identified ISOCAM sources in our fields. Completeness limits (estimated from expected MIR fluxes of NIR stars) are 1.5 mJy and 2 mJy for the LW2 and LW3 bands, while sources down to 0.7 and 1.0 mJy, respectively, are detected. All of the high-reliability LW2 sources and 84 per cent of the high-reliability LW3 sources are identified in the NIR. The detection efficiencies for identified

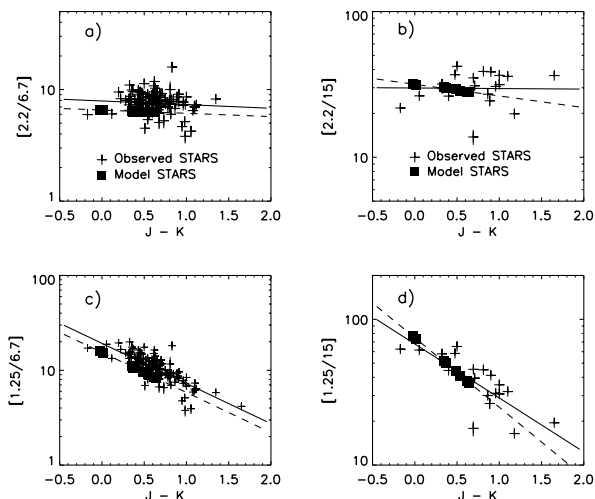


Figure 1. Stars in NIR/MIR vs.  $J - K$  diagram. The  $6.7$  and  $15\mu\text{m}$  fluxes of the ELAIS v.1.3 catalogue stars (crosses) are in ADUs. The model colours (filled squares, in mJy) have been calculated from stellar spectra templates used in the ISOCAM calibration program. The solid and dashed lines are fits to the observed data and model points, respectively. Constant correction factors for the ADU to mJy conversion are derived from these fits.

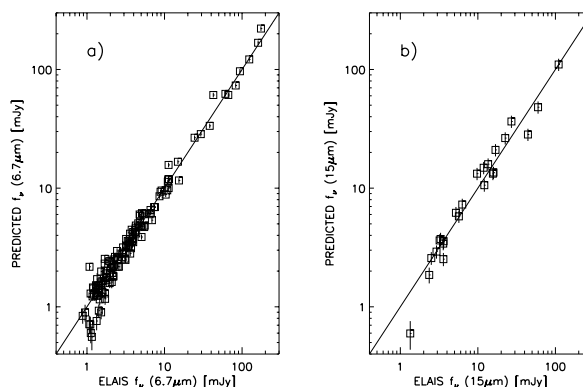


Figure 2. Predicted stellar fluxes vs. the observed ELAIS fluxes.

$R=3$  sources are lower, and the overall ISOCAM v.1.3 catalogue NIR percentages become 97 and 55 per cent at LW2 and LW3, respectively. 53 sources are common to both ISOCAM filters, and 29 of these turn out to be galaxies.

It is interesting to note the overall proportions of stars and galaxies: in the near- and mid-IR matched catalogue 81 per cent of the  $6.7\mu\text{m}$  sources are stars. At  $15\mu\text{m}$  only 21 per cent of the objects are stars.

### 4.2. INFRARED COLOURS OF GALAXIES

In general, the emission from galaxies in near-IR bands is due to the stellar contribution, the  $6.7\mu\text{m}$  carries information on the PAH contribution, and any strong  $15\mu\text{m}$  emission would indi-

<sup>1</sup> see [http://www.iso.vilspa.esa.es/users/exp\\_lib/ISO/wwwcal/cam.html/](http://www.iso.vilspa.esa.es/users/exp_lib/ISO/wwwcal/cam.html/)

Table 1. ISOCAM sources in the 1 sq.deg. near-IR survey area within the ELAIS N1 and N2 fields, per band and reliability parameter; R=2 stands for a ‘secure’ detection and R=3 for a ‘probable’ detection. Column (Det.) refers to the total number of ISO sources and (Ident.) to the number of NIR identifications.

		Det.	Ident.	Stars	Gals.
N1					
LW3	R=2	47	37	7	30
	R=3	59	12	1	11
N2					
LW2	R=2	170	170	141	29
	R=3	53	47	34	13
LW3	R=2	68	60	19	41
	R=3	115	49	6	43
LW2&3	R=2&3	53	53	24	29
TOTALS					
LW2		223	217	175	42
LW3		289	158	33	125

cate warm dust. Several colour indices may thus be useful in studying the relative strengths of these components and processes in galaxies.

Fig. 3 shows the 6.7 and 15  $\mu\text{m}$  fluxes of those galaxies in our sample which are detected in both MIR bands, normalized with the  $K$ -band flux, i.e. by the stellar contribution to the brightness of the galaxy. Since the  $K$ -band is well correlated with the mass of the galaxy, this normalization also corrects for mass-luminosity dependence to first order. GRASIL models (Silva et al. 1998) for different Hubble types are overplotted, with redshift dependence from  $z=0$  (large symbol) to  $z=1$  (open end of curve). The strengths of the mid-IR fluxes are seen to correlate strongly, and the difference in the relative strength of mid-IR flux ranges nearly two orders of magnitude.

The colour-colour plot is divided into four different regions using template colours of local ISO-galaxies and models. Using a comparison sample of ISO-galaxies from the literature (Boselli et al. 1998, Dale et al. 2000, Roussel et al. 2001a) we verified that the types of galaxies become systematically later upward along the diagonal – however the NIR/MIR is not a good indicator of Hubble type if the galaxy has  $[6.7/15]$ -ratios much less than unity (i.e. strong star formation, see below). Most of our sources group in the low-redshift,  $z = 0.1 - 0.4$ , late type galaxy region.

The two mid-IR filters detect surprisingly different populations. Only one third of LW3 galaxies are detected in LW2 and two thirds of LW2 galaxies are detected in LW3. Using arguments from detection limits and expected colours of sources, it is clear that faint late type spirals and starbursts make up the majority of LW2-missed sources. Most of the galaxies missed by the LW3-band are early types with high a  $[2.2/6.7]$ -ratio.

#### 4.3. MIR AND NIR AS STAR FORMATION TRACERS

The use of MIR fluxes and the  $[6.7/15]$  ratio as star formation tracers has been recognized over the past few years. In Fig. 3, a

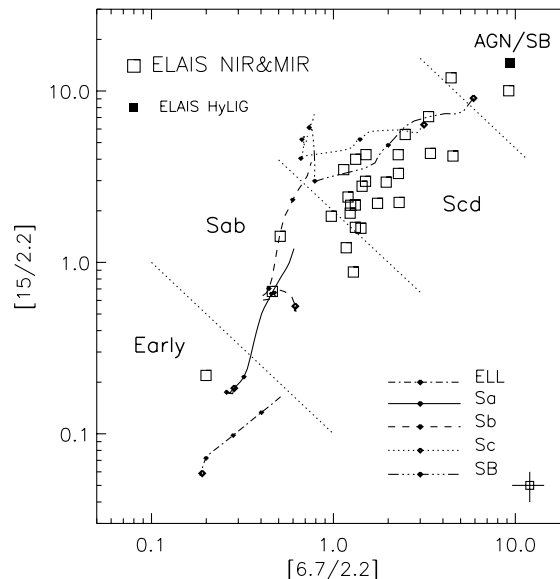


Figure 3. The 6.7 and 15  $\mu\text{m}$  fluxes of our ELAIS galaxies normalized with the  $K$ -band flux. Curves show models adopted from the GRASIL library and the dotted lines roughly separate areas for different types of galaxies. A hyper-luminous IR-galaxy detected in another ELAIS region (Morel et al. 2001) is also shown (solid symbol).

departure upward from the one-to-one  $[6.7/15] = 1$  diagonal is a measure of star forming activity, i.e. galaxies with  $[6.7/15] < 1$  are most active. The ELAIS galaxies yield an average mid-IR flux ratio  $[6.7/15] = 0.67 \pm 0.27$ .

Roussel et al. (2001b) found a good correlation between MIR emission and  $H\alpha$ , and thus star formation rate (SFR). Adopting relations therein, and assuming a typical redshift of  $z = 0.2$  for the late-type galaxies in our sample, we estimate average SFRs of  $\sim 15 - 30 M_{\odot}/\text{yr}$  for these galaxies.

Using the same comparison sample mentioned in Section 4.2 and the well known IRAS  $[60/100]$  tracer, we checked how the MIR and NIR/MIR flux ratios might trace star formation and activity level of galaxies.

Galaxies from literature are plotted in Fig. 4. First of all, the  $[2.2/15]$  value (anti)correlates closely with  $[60/100]$ . The  $[2.2/15]$  colour thus also indicates the activity level of galaxies.

Also, one can see that the  $[6.7/15]$  stays constant at low  $[60/100]$  but drops at higher heating levels (i.e. high  $[60/100]$ ). This has been noted before (eg. Dale et al. 2000) and has been understood as the rising emission from the very small grains entering the 15  $\mu\text{m}$  band. However, since the  $[2.2/15]$  does not have a corresponding break in its slope, this can not be the only explanation. Since there is a break in the  $[2.2/6.7]$  slope, a flattening beyond  $[60/100] \sim 0.4$ , the destruction of the PAH emission carriers in this MIR regime is indicated. The ISO-IRAS diagram, i.e. the  $[6.7/15]$  vs.  $[60/100]$ , must then be explained by both the increasing 15  $\mu\text{m}$  emission and relatively decreasing 6.7  $\mu\text{m}$  emission.

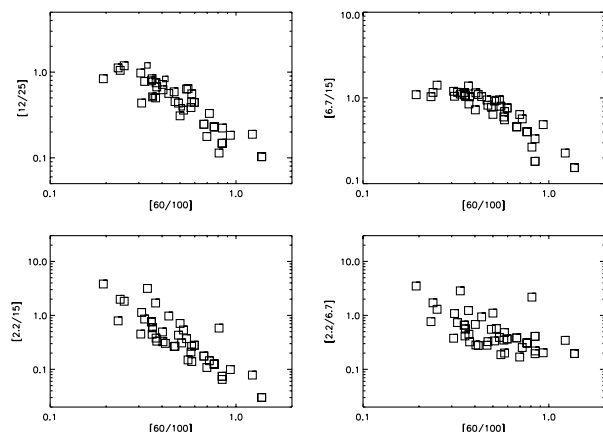


Figure 4. Comparing the IRAS [60/100] colour and star-formation tracer to near- and mid-IR colours. *E/S0* galaxies are excluded from this plot.

## 5. SUMMARY

We have presented photometry of a subsample of the ISOCAM ELAIS survey from the N1 and N2 fields. The near- and mid-IR stars detected in the field were used to perform an accurate new calibration of the ELAIS ISOCAM data at both 6.7 and 15  $\mu\text{m}$ .

Excluding the stars, the mid-IR survey as a whole mainly detects late type spiral galaxies and starbursts. The faintest population of these is missed by the LW2 filter. The few objects missed by the longer mid-IR filter are most probably early type galaxies. Simple arguments indicate that typical redshifts of the sample seen with both mid-IR bands are  $z \approx 0.2$ .

NIR/MIR colour-colour plots are useful in studying the relative emission strengths of stellar, PAH, and warm dust components in galaxies. In a [15/2.2] vs. [6.7/2.2] plot the Hubble type of a galaxy can be roughly estimated from its position along the diagonal.

Star formation activity can also be estimated. In this same [15/2.2] vs. [6.7/2.2] plot the quiescent galaxies fall on the diagonal where  $[6.7/15] \approx 1$ . Increasing star formation activity raises the galaxies above the one-to-one curve, i.e.  $[6.7/15] < 1$ . Comparing with the IRAS [60/100] colour, we have shown that the  $[6.7/15]$  drops at high heating levels, and that this is a result of both increasing 15  $\mu\text{m}$  emission and the destruction of the carriers of PAH emission seen in the ISOCAM 6.7  $\mu\text{m}$  band.

## ACKNOWLEDGEMENTS

We gratefully acknowledge the work done by the whole ELAIS collaboration – we particularly made use of the data sets made available by colleagues at Imperial College.

## REFERENCES

Blommaert, J., 1998, ‘ISOCAM Photometry Report V2.1.1’, [http://www.iso.vilspa.esa.es/users/expl\\_lib/CAM/](http://www.iso.vilspa.esa.es/users/expl_lib/CAM/)

photom\_rep.fn.ps.gz  
 Boselli, A., et al., 1998, *A&A*, 335, 53  
 Cesarsky, D., et al., 1996, *A&A*, 315, L309  
 Dale, D.A., et al., 2000, *AJ*, 120, 583  
 Genzel, R., Cesarsky, C.J., 2000, *ARAA*, 38, 761  
 Helou, G., 1999, in Cox, P., Kessler, M.F., eds., *ESA SP-47, The Universe As Seen by ISO*, ESA Publ.Div., ESTEC, Noordwijk, p. 797  
 Helou, G., Lu, N.Y., Werner, M.W., Malhotra, S., Silbermann, N., 2000, *ApJ*, 532, L21  
 Mattila, K., Lehtinen, K., Lemke, D., 1999, *A&A*, 342, 643  
 Morel, T., et al., 2001, *MNRAS*, 327, 1187  
 Oliver S., et al., 2000, *MNRAS*, 316, 749  
 Roussel, H., et al., 2001a, *A&A*, 369, 473  
 Roussel, H., et al., 2001b, *A&A*, 372, 427  
 Sauvage, M., et al., 1996, *A&A*, 315, L89  
 Serjeant S., et al., 2000, *MNRAS*, 316, 768  
 Silva, L., et al., 1998, *ApJ*, 509, 103  
 Väisänen, P., et al., 2000, *ApJ*, 540, 593  
 Väisänen, P., et al., 2002, *MNRAS*, in press (astro-ph/0208412)  
 Vigroux, L., et al., 1996, *A&A*, 315, L93  
 Vigroux, L., et al., 1999, in Cox, P., Kessler, M.F., eds., *ESA SP-47, The Universe As Seen by ISO*, ESA Publ.Div., ESTEC, Noordwijk, p. 805